

Article

Shaking Rate during Production Affects the Activity of *Escherichia coli* Surface-Displayed *Candida antarctica* Lipase A

Chen-Fu Chung ¹, Shih-Che Lin ¹, Tzong-Yuan Juang ^{2,*}  and Yung-Chuan Liu ^{1,*} 

¹ Department of Chemical Engineering, National Chung Hsing University, Taichung 402, Taiwan; hahahaandy@gmail.com (C.-F.C.); leo83873@yahoo.com.tw (S.-C.L.)

² Department of Cosmeceutics, China Medical University, Taichung 40402, Taiwan

* Correspondence: tyjuang@mail.cmu.edu.tw (T.-Y.J.); ycliu@dragon.nchu.edu.tw (Y.-C.L.)

Received: 5 March 2020; Accepted: 30 March 2020; Published: 1 April 2020



Abstract: In this study, a surface-display system was applied for the expression of lipase A in an *E. coli* expression system. Since the target protein was exposed on the cell membrane, the shaking rate during culturing might have increased the oxygen mass transfer rate and the shear stress, both of which would be detrimental to the surface-displayed protein. The shaking rate did indeed have an effect on the properties of the surface-displayed lipase A from *Candida antarctica* (sdCALA). When cultivated at a shaking rate of less than 50 rpm, the specific activity of sdCALA was low, which was due to the limited amount of dissolved oxygen. When the shaking rate was greater than 100 rpm, the specific activity decreased as a result of shear stress. When cultivating CALA and sdCALA at various temperatures and values of pH, both proteins displayed the same activity profile, with the optimum conditions being 60 °C and pH 6. A kinetic study revealed that the sdCALA cultivated at 100 rpm gave a higher value of v_m (0.074 $\mu\text{mol}/\text{mL}/\text{min}$) and a lower value of K_m (0.360 $\mu\text{mol}/\text{mL}$) relative to those obtained at 200 rpm and relative to those of the free CALA. sdCALA retained over 80% of its activity after treatment at 70 °C for 30 min, but its activity decreased rapidly when the temperature was above 80 °C. The specific activity of sdCALA decreased in the presence of acetonitrile and acetone relative to that of the control (50% ethanol), regardless of the solvent concentration. The highest activity (0.67 U/mL) was obtained when the ethanol concentration was 30%.

Keywords: *Candida antarctica* lipase A; surface-display system; shear rate; mass transfer rate; enzymatic kinetic study

1. Introduction

Candida antarctica is a psychrophilic Basidiomycetous yeast originally selected from a strain found in Antarctic habitats. This strain expresses two lipolytic enzymes displaying different catalytic properties: *Candida antarctica* lipase A (CALA) and lipase B (CALB) [1]. CALB, first described in 1994 [2], has a molecular weight of approximately 34–43 kDa. As a result of its high selectivity toward secondary alcohols and its endurance in organic solvents and at high temperatures [2,3], it has been widely applied industrially and academically. The structure of CALA was solved using X-ray crystallography [2,4], with a molecular weight of approximately 45–53 kDa. Compared with CALB, the properties of CALA have been less well explored. CALA displays specific hydrolytic properties; for example, it retains its activity at high temperature (>70 °C) and in acidic environments. In addition, CALA preferentially hydrolyzes triglycerides at position sn-2, which is located at the center of the carbon chain; therefore, it has been applied in the preparation of fat substitutes and to the development of new modes of drug delivery [5]. At present, other microorganisms known to

produce CALA include *Aspergillus sp.* [6] and *Pichia sp.* [2,7] fungi and prokaryotic *E. coli* [8]. Studies of CALA have mainly been focused on its use in different host cells [9], food processing [10], and transesterification [10,11]. To render CALA more applicable, new processes should be developed for its rapid and efficient production.

In 1985, Smith inserted the recombinant antigens to the N-terminus of the filamentous bacteriophage coat protein pIII and expressed them on the phage surface [12]. Many carrier proteins have been demonstrated to carry the protein outside the membranes of cells. Common carrier proteins include S-layer protein, lipoprotein, bacterial fimbriae, and ice nucleation protein (INP) [10,13,14]. A variety of biotechnological processes and materials—for example, antibody production, bioconversion, biosensors, bioadsorbents, and oral vaccines—have adopted this technique for process improvement [13,14].

INP is a membrane-bound protein that is capable of binding to the phospholipids of cell membranes [15,16]. The main structure of INP can be divided into three parts: the N-terminus, a hydrophobic region that binds to the phospholipids of the outer membrane; an intermediate region, comprising mainly AlaGlyTyrGlySerThrLeuThr (AGYGSTLT) repeat fragments that form an ice core; and the C-terminus, which is a hydrophilic region that can link with the target protein and expose it to the outer membrane surface. INP-based systems can suitably express recombinant protein molecules after modulating the length of the intermediate repeat region, thereby minimizing the issue of steric disorder [17]. According to its genotypes, INP can be classified into four systems: *inaK* [18], *inaQ* [19], *inaV* [20], and *inaX* [21]. The expression of INP is most stable during the stationary phase of culturing. INP-based systems are among the most useful for Gram-negative bacteria surface-display applications [18].

Many genetic engineering technologies require cell surface carriers for the rapid expression of foreign proteins. Through the surface expression of lipases, for example, various surface-display lipases have been developed with the goal of applying them directly to lipolytic reactions. Matsumoto et al. constructed a yeast cell surface-display system for lipase expression, using a flocculation functional domain of Flo1p as the carrier [22]. Moura et al. assessed the biochemical features of lipase B when immobilized on the cell surface of the methylotrophic yeast *Pichia pastoris*, using the yeast surface-display approach [23]. Liu et al. displayed lipase Lip2 from *Yarrowia lipolytica* on the cell surface of *Saccharomyces cerevisiae*, using Cwp2 as an anchor protein; the thermostability of the displayed lipase was superior to that of free lipase Lip2 [24].

The use of recombinant *E. coli* to express intracellular target proteins is common. The main issue hindering its application has been the separation and purification of the target protein from the harvested cultural broth—a tedious and labor-intensive process that increases the complexity of production. Surface-display systems could provide an alternative means of obtaining enzymes for direct industrial applications. Wilhelm et al. demonstrated that the cell surface-display protein LipH from *P. aeruginosa* could properly express foldase–lipase complexes on the surface of *E. coli* cells [25]. Jo et al. displayed the lipase from *Bacillus licheniformis* ATCC14580 on the cell surface of *E. coli* by using Lpp'OmpA as the anchoring protein; this development suggested that *E. coli*, through the direct display of lipase on its cell membrane, could be applied as a whole cell biocatalyst [26].

In this present study, we constructed an INP surface-display system to express lipase A in the *E. coli* outer membrane. Although some articles describe the expression of lipase anchoring on the *E. coli* cell membrane [25,26], those studies did not focus on the effects of cultivation on the biochemical features of surface-display CALA (sdCALA). For example, mass transfer and shear stress during cultivation might directly affect the properties of the enzyme through its exposure to the outside environment. To test this concept, here we performed a preliminary comparison of the biochemical properties of CALA produced intracellularly with those of sdCALA anchored on the membrane. In addition, we also evaluated the kinetic properties of sdCALA prepared under various cultivation conditions.

2. Results and Discussion

2.1. Gene Construction and Protein Expression

The host strains *E. coli* JM109 (DE3)/pET22b-calawt and *E. coli* JM109 (DE3)/pINP-CALA were constructed according to the methods listed in Section 3.2. Both types of cells were cultivated and induced according to the methods listed in Section 3.3. To obtain the intracellular CALA, the cells were disrupted through sonication, followed by centrifugation to collect the supernatant containing CALA. To obtain sdCALA, the collected cells were dissolved in the same volume of sodium phosphate buffer (pH 6.0) for further use. Sodium dodecyl sulfate–polyacrylamide gel electrophoresis (SDS-PAGE) was performed to check for the correct expression of intracellular and surface-display CALA (Figure 1). In the PAGE gel, a band in Lane 1 revealed the successful expression of CALA (53 kDa) and that the expression was mainly intracellular as the soluble protein (Lane 2). In addition, no clear band at 53 kDa appeared in the pellets (Lane 3), implying that no inclusion body was formed. For the surface expression system, a band for INP-CALA (80 kDa) appeared in Lane 4, confirming the accurate expression of the fusion protein INP-CALA (Lane 4), with the main expression located at the pellet (Lane 6) with only a very unclear band in Lane 5. Thus, the expression of sdCALA occurred mainly on the cell pellet.

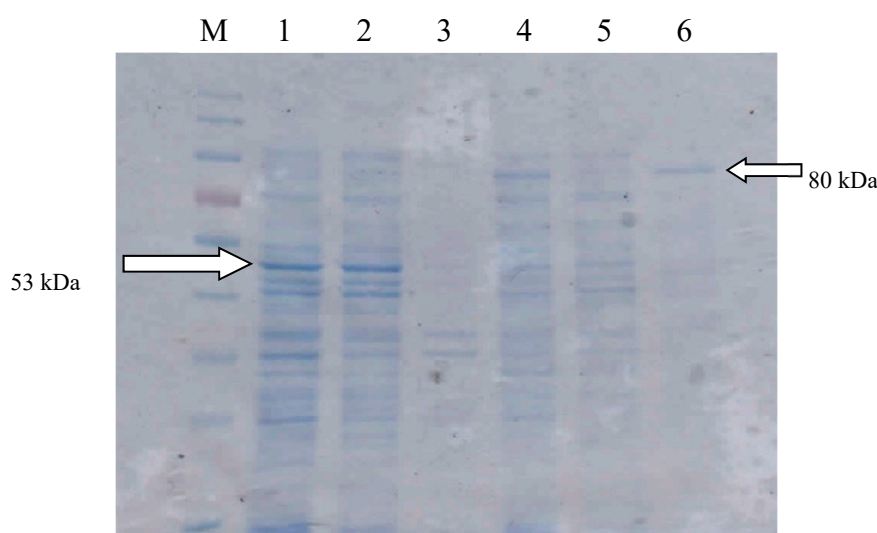


Figure 1. SDS-PAGE of intracellular *Candida antarctica* lipase A (CALA) and surface-display CALA. Lane M: Marker; Lanes 1–3: Whole cells, supernatant, and pellet of intracellular CALA, respectively; Lanes 4–6: Whole cells, supernatant, and pellet for surface-display CALA (sdCALA), respectively.

The activities of the CALA enzymes obtained from the two systems were assayed (Table 1). The activity of CALA obtained from the intracellular system was approximately 0.326 U/mL, while that from the surface expression system was 0.285 U/mL. The specific activity of sdCALA (0.285 U/mg) was larger than that of CALA (0.251 U/mg). We suspected that sdCALA on the cell membrane might have had a larger space for its proper extension. Although the volumetric activity of the lipase A produced through surface expression was slightly lower than that of the intracellular system, the higher specific activity and avoidance of cell disruption suggest that it might be convenient in certain applications. In addition, we found, interestingly, that a small amount of soluble fusion protein INP-CALA existed in the periplasm, with a relative activity of 0.057 ± 0.04 U/mL. The total expression of sdCALA with the supernatant plus pellet would compete with that of the intracellular CALA.

Table 1. Expression and activities of intracellular CALA and surface-displayed CALA.

Expression System	Biomass (mg/mL)	Activity (U/mL)	Specific Activity (U/mg)
Intracellular ^a (pET22b-calawt)	1.298 ± 0.232	0.326 ± 0.11	0.251 ± 0.047
Surface display ^b (pINP-CALA)	0.999 ± 0.052	0.285 ± 0.07	0.285 ± 0.013

^a To measure the volumetric activity of CALA, the supernatant obtained as stated in Section 3.3 was used for the assay. ^b To measure the volumetric activity of sdCALA, the harvested cells were resuspended in the same volume of phosphate buffer (pH 6.0) for the assay.

In our laboratory, we have frequently applied INP to expose outer membrane proteins; some papers concerning this approach have been published [27–30]. The most typical use has been in the expression of INP-INT-EGFP (INP-intein-enhanced green fluorescent protein) outside the cell membrane and then, through the self-cleavage of INT, to relieve the EGFP to the supernatant [30]. In such a case, the expression of EGFP as the outer membrane protein would result in a green-colored cell pellet. In addition, this approach has also been used for the expression of D-hydantoinase outside the cell membrane and to simplify the enzyme purification process [28]. Those previous studies demonstrated that INP could be used not only to correctly express the target protein as an outer membrane protein but also to maintain the correct conformation of the protein and its usual activity (measured through a whole-cell activity assay). In this study, we used INP to express lipase A as an outer membrane enzyme and applied a tributyrin agar plate test to demonstrate the existence of outer membrane INP-CALA, as described in Section 3.6. Figure 2 displays the results. In the case of sdCALA, a clear zone formed around the cell colony, which was due to direct hydrolysis of the tributyrin. In contrast, the cells prepared with the intracellular CALA did not form any such clear zone. Thus, the JM109/pINP-CALA system could indeed express sdCALA properly outside the cell membranes.

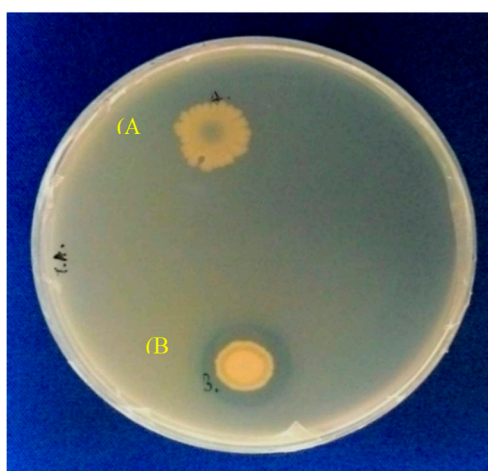


Figure 2. Tributyrin plate tests for intracellular and surface-display CALA. (A: Intracellular CALA; B: sdCALA).

2.2. Effect of Shaking Rate on sdCALA Activity and Biomass

Since the expressed sdCALA was anchored outside the cell membrane, the cultivation conditions—especially the shaking rate—would presumably induce various mass transfer rates and shear rates on the produced enzyme. To examine this concept, sdCALA production was performed with cultivation at various shaking rates (Figure 3). The shaking rate did indeed affect the enzyme specific hydrolysis activity and biomass production. The biomass increased remarkably upon increasing the shaking rate from 50 to 100 rpm, but the increases were less dramatic thereafter. The specific activity also greatly increased upon increasing the shaking rate from 50 to 100 rpm. However, when the shaking rate was at or above 150 rpm, the specific activity decreased significantly. To tests the effects of mass transfer and shear on the biomass production and lipase activity, relevant data were

calculated according to Equations (1)–(5), as described in Section 3.4, and these are listed in Table 2. At the low shaking rate of 50 rpm, a low rate of oxygen mass transfer would occur, limiting cell growth and resulting in very low biomass production. This limited oxygen transfer rate would also block the proper expression of sdCALA. When the shaking rate was 100 rpm, the higher rate of oxygen mass transfer would benefit cell growth, resulting in a high expression of sdCALA. When the shaking rate was 150–200 rpm, the higher rates of oxygen mass transfer would slightly increase the biomass production, but high shear rates would have a detrimental effect on the expression of sdCALA, due to its direct exposure to the broth. To minimize the damage caused at high shear rates, we selected a shaking rate of 100 rpm for subsequent expressions of sdCALA.

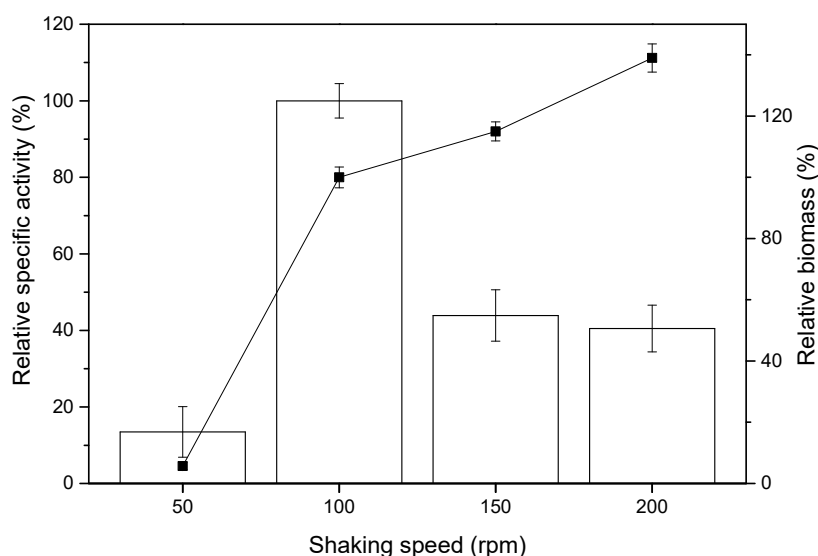


Figure 3. Effect of shaking rate on the specific activity (bars) and biomass production (black squares) of sdCALA. To calculate relative values, the value measured at 100 rpm was set as 100%.

Table 2. Effect of mass transfer and shear rate on the specific activity and biomass production of sdCALA.

Shaking Rate (rpm)	K_{La} (h^{-1})	γ (h^{-1})	Relative Specific Activity (%)	Relative Biomass (%)
50	9.6	13	13.5 ± 6.6	5.7 ± 1.2
100	21.4	89	100 ± 4.5	100 ± 3.4
150	34.2	276	43.9 ± 6.7	115 ± 3.1
200	47.8	617	40.5 ± 6.1	139 ± 4.6

2.3. Optimal Temperature and pH for Production of CALA and sdCALA

In reactions involving biocatalysts, the enzyme activity would increase upon increasing the temperature within a certain range. However, the activity would decrease if the temperature was too high, due to the effect of enzyme denaturing. For example, most lipolytic enzymes lose their activity when the temperature exceeds 40 °C [31]. For CALA, a thermophilic lipolytic enzyme [32,33], the optimal temperature has been reported to be in the range from 50 to 70 °C [33,34] and possibly even as high as 90 °C [33]. We prepared two types of sdCALA through the cultivation of JM109/pINP-CALA at 100 and 200 rpm (denoted herein as sdCALA100 and sdCALA200, respectively). As references, we also prepared two samples of intracellular CALA enzymes from cultures of JM109/pET22b-calawt under the same conditions (CALA100 and CALA200, respectively). The activities of all of these tested enzymes were adjusted to 0.35 U/mL using 50 mM phosphate buffer (pH 6).

Figure 4 displays the effect of temperature on the activities of CALA and sdCALA. All of the enzymes exhibited the same profile in response to the temperature. The optimal temperature was 60

°C in each case. Thus, even though they had been subjected to different culture conditions and various expression systems, the resulting enzymes exhibited the same dependency on temperature.

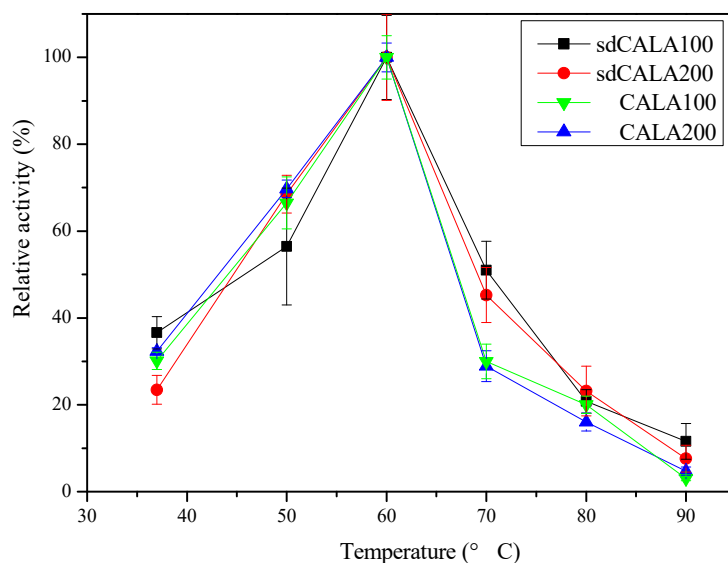


Figure 4. Effect of temperature on the relative activities of samples of CALA and sdCALA prepared at different shaking rates.

Various lipases have their own operating pH ranges, from as low as pH 3 to as high as pH 9 [35,36]. Since the structure of the active site might be affected by the pH, a lipase might display acid- or alkali-resistant properties. Figure 5 displays the effect of pH on the activities of the CALA and sdCALA samples prepared at the two spinning rates. All of these enzymes had the same pH-dependency, with the optimal activities occurring at pH 6. The activities decreased sharply when the pH was 7, and the enzymes were almost inactive at pH 9. Thus, we conclude that CALA is not an alkaline enzyme. Furthermore, the use of different shaking rates for the expression of CALA and sdCALA did not have any effect on their pH dependency.

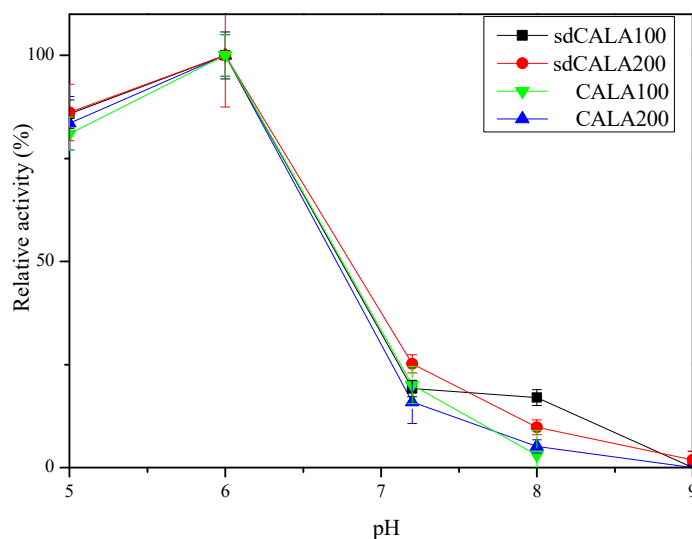


Figure 5. Effect of pH on the relative activities of CALA and sdCALA samples prepared at different shaking rates.

2.4. Kinetic Analyses of Various CALA Enzymes

We adopted the Michaelis–Menten kinetics model in Equation (6) to test the kinetic behavior of our various lipase A enzymes. Figure 6 presents a Hanes–Wolf plot of the substrate concentration divided by the activity with respect to the substrate concentration (Equation (7)). The kinetic parameters for each enzyme were collected through linear fitting of the data. Table 3 lists the calculated values of K_m and v_m . All of the enzymes displayed values of v_m in range of 0.059–0.072 ($\mu\text{mol}/\text{mL}/\text{min}$) and K_m in range of 1.032–1.821 ($\mu\text{mol}/\text{mL}$), except for sdCALA100, which had a slightly higher value of v_m (0.074 $\mu\text{mol}/\text{mL}/\text{min}$) and a much lower value of K_m (0.360 $\mu\text{mol}/\text{mL}$). Thus, preparing sdCALA at 100 rpm significantly improved both its reaction rate (high v_m) and substrate affinity (low K_m). The sdCALA obtained at 200 rpm gave a value of K_m close to those of the intracellular enzymes. Notably, the collection of intracellular enzymes requires harsh sonication or high pressures for cell disruption, potentially influencing the properties of the enzymes and decreasing the affinity to the substrate. Furthermore, we suspect that sdCALA200, which had been subjected to a higher shaking rate and a higher shear rate, had poorer affinity than sdCALA100 toward the substrate. Therefore, such kinetic analysis can provide indirect evidence for the shear rate affecting the performance of CALA prepared under various cultivation conditions.

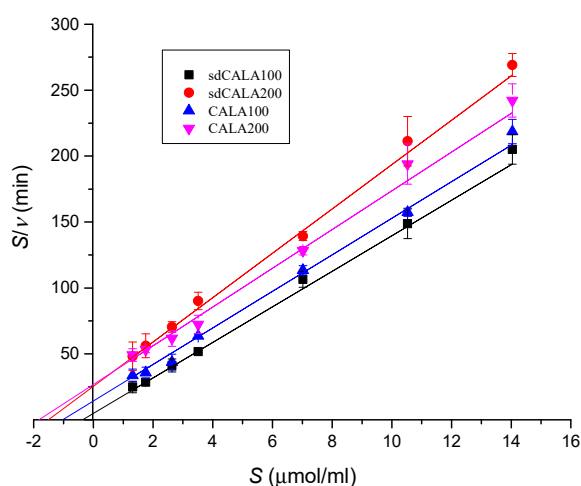


Figure 6. Hanes–Wolf diagram for CALA and sdCALA.

Table 3. Kinetics parameters of CALA and sdCALA.

Lipase	v_m ($\mu\text{mol}/\text{mL}/\text{min}$)	K_m ($\mu\text{mol}/\text{mL}$)
sdCALA100	0.074	0.360
sdCALA200	0.059	1.510
CALA100	0.072	1.032
CALA200	0.068	1.821

2.5. Thermal Stability of sdCALA

We tested the thermal stability of sdCALA100 at various temperatures. Samples were taken every 10 min to obtain the activity assay at the optimal temperature of 60 °C. Figure 7 reveals that sdCALA retained greater than 80% of its activity when heated at a temperature lower than or equal to 70 °C for 30 min; however, at 80 °C, its activity dropped remarkably, to less than 20% after 30 min, and it was almost completely lost after being heated at 90 °C for 10 min. We found in our earlier study of the optimal temperature that the relative activity of sdCALA decreased to less than 50% when it was in contact with 50% ethanol (in the activity assay) at 70 °C for 5 min; however, in this stability test, greater than 80% of the residual activity remained after heating at 70 °C for 30 min in the absence of contact with ethanol. Thus, a high concentration of ethanol presumably had a negative effect on the activity of

sdCALA. Accordingly, we tested the influence of various organic solvents at various concentrations on the hydrolysis reactions of sdCALA.

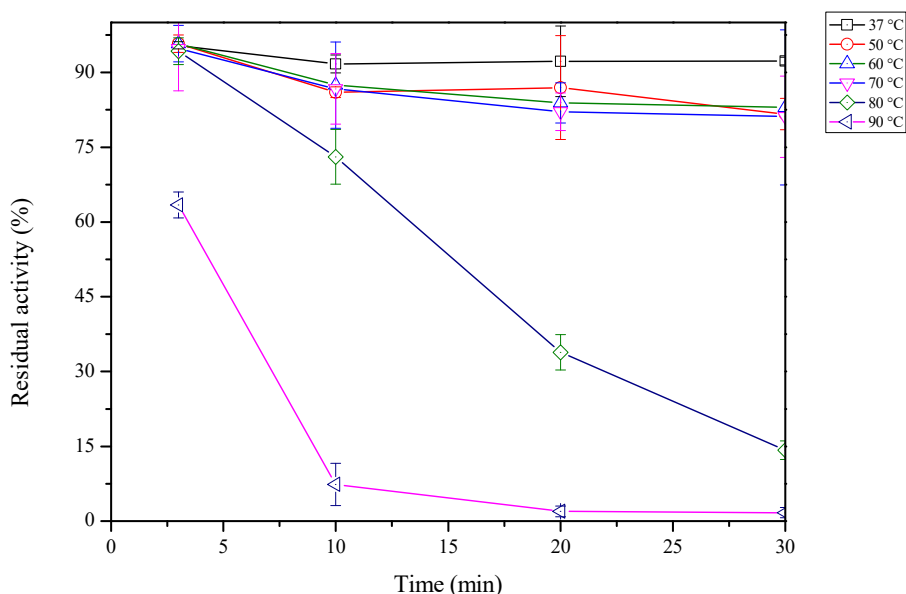


Figure 7. Thermal stability tests for sdCALA, where the initial activity was set as the control.

2.6. Effect of Organic Solvents on sdCALA Activity

Yang et al. studied the effects of various organic solvents on the activity of purified CALA produced by *Pichia pastoris* [37]. They found that when CALA was treated with acetonitrile or acetone, its activities toward esterification and hydrolysis increased. However, when treated with ethanol, only 20% of the lipolytic activity remained; when treated with isopropanol, 20% of the hydrolysis and esterification activities were lost.

To explore the effects of organic solvents on sdCALA, we applied ethanol, acetonitrile, acetone, and isopropanol at various concentrations as replacements for 50% ethanol and analyzed the activities (Figure 8). The activity obtained in the presence of 50% ethanol was set as the control (100%). When the concentration of ethanol decreased to 30%, the activity of sdCALA increased significantly, but it decreased upon lowering the concentration thereafter, which was possibly because of the low solubility of the substrate [*p*-nitrophenyl palmitate (*p*-NPP)] at such low concentrations of ethanol. In the case of isopropanol, the activity increased upon decreasing the concentration of the organic solvent, but all of the activities were lower than that of the control (50% ethanol), except when the concentration of isopropanol was at or below 30%. The results obtained when using acetonitrile or acetone were quite different. Increasing the concentration of either of these organic solvents from 20% to 40% enhanced the activity, but a concentration of 50% had a negative effect. Nevertheless, all of the activities in the presence of these two solvents were lower than that of the control. Thus, the results of this study were quite different from those reported by Yang et al. [37]. Presumably, the organic solvents affected the conformation of CALA, exposing its active site more to the substrate. On the other hand, the organic solvents might also have decreased the activities through denaturing of the structure of CALA. In the case of sdCALA, the host *E. coli* might also have been a factor, which was subjected to its own solvent effect—the organic solvents might have varied the cell membrane structure and indirectly affected the structure of the anchored CALA [38,39]. A more detailed study of the effect of solvents on hosts would be worthy in future.

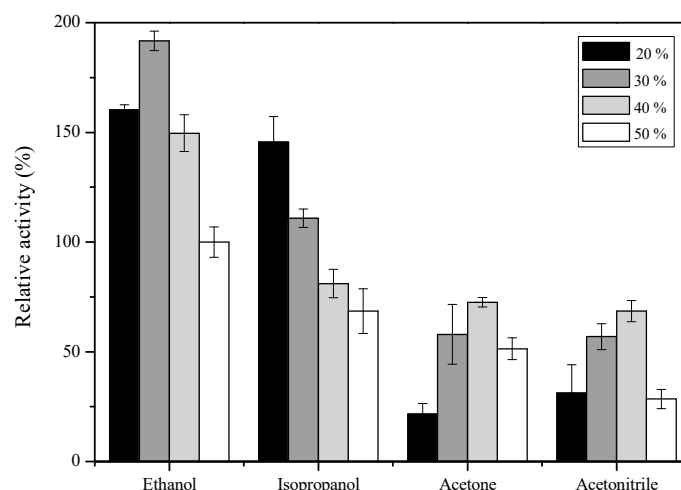


Figure 8. Effect of the concentrations of various organic solvents on the activity of sdCALA with 50% ethanol set as the control.

3. Materials and Methods

3.1. Strains, Plasmids, and Source

E. coli DH5 α and *E. coli* JM109 (DE3) were used as host cells for gene transfer and recombinant protein expression, respectively. The plasmid pET22b-calawt containing the CALA(*cala*) gene sequence was a gift from Professor Bornscheuer at Greifswald University, Germany; the pET28a-*inaX* having the INP(*inaX*) gene was provided by Professor Wen-Teng Wu of National Cen Kong University, Taiwan. The *E. coli* host strains and vectors used in this study are listed in Table 4. All other chemicals were of analytical grade and obtained from a local supplier.

Table 4. *E. coli* strains and plasmids used in this study. INP: ice nucleation protein.

Strain or Plasmid	Genotype and Relevant Characteristics	Source
DH5 α	F- endA1 glnV44 thi-1 recA1 relA1 gyrA96 deoR nupG Φ 80dlacZ Δ M15 Δ (lacZYA-argF)U169, hsdR17(rk – mk +), λ -	Novagen
JM109 (DE3)	endA1 glnV44 thi-1 relA1 gyrA96 recA1 mcrB+ Δ (lac-proAB) e14- (F' traD36 proAB+ lacIq lacZ Δ M15) hsdR17(rk – mk +) λ (DE3)	NEB
pET22b-calawt	CALA (<i>cala</i>) gene fragment in pET22b	Professor Bornscheuer (Greifswald University, Germany)
pET26b- <i>inaX</i>	INP (<i>inaX</i>) gene fragment in pET26b	Professor Wu (NCKU, Taiwan)
yT&A	pBluescript IISK(-) with modified MCS	Yeastern Biotech

3.2. Construction of Expression Systems

pET22b-calawt was used as the template to amplify the *cala* gene with restriction sites of *EcoRI* and *XhoI*. The primers are listed in Table 5. The obtained inserts (PCR products) were further ligated to vector yT&A (Yeastern Biotech) to build the constructs of pT-CALA. The *cala* gene was cut from pT-CALA via the restriction enzyme sites of *EcoRI* and *XhoI* and was ligated into pET26b-INP to form the pINP-CALA construct (Figure 9). The production strains were prepared via heat-shock, transforming the respective pET22b-calawt and pINP-CALA into the host *E. coli* JM109 (DE3). All recombinant DNA manipulations were performed using standard procedures [40].

Table 5. Primers used in this study.

Primer Name	Primer Sequence (5'3')	Template
CALA-F	GAATTCATGCGTGTGAGCCTGCGTAG (<i>EcoRI</i>)	pET22b-calawt
CALA-R	CACTCGAGCACCACCACCA (<i>XhoI</i>)	pET22b-calawt

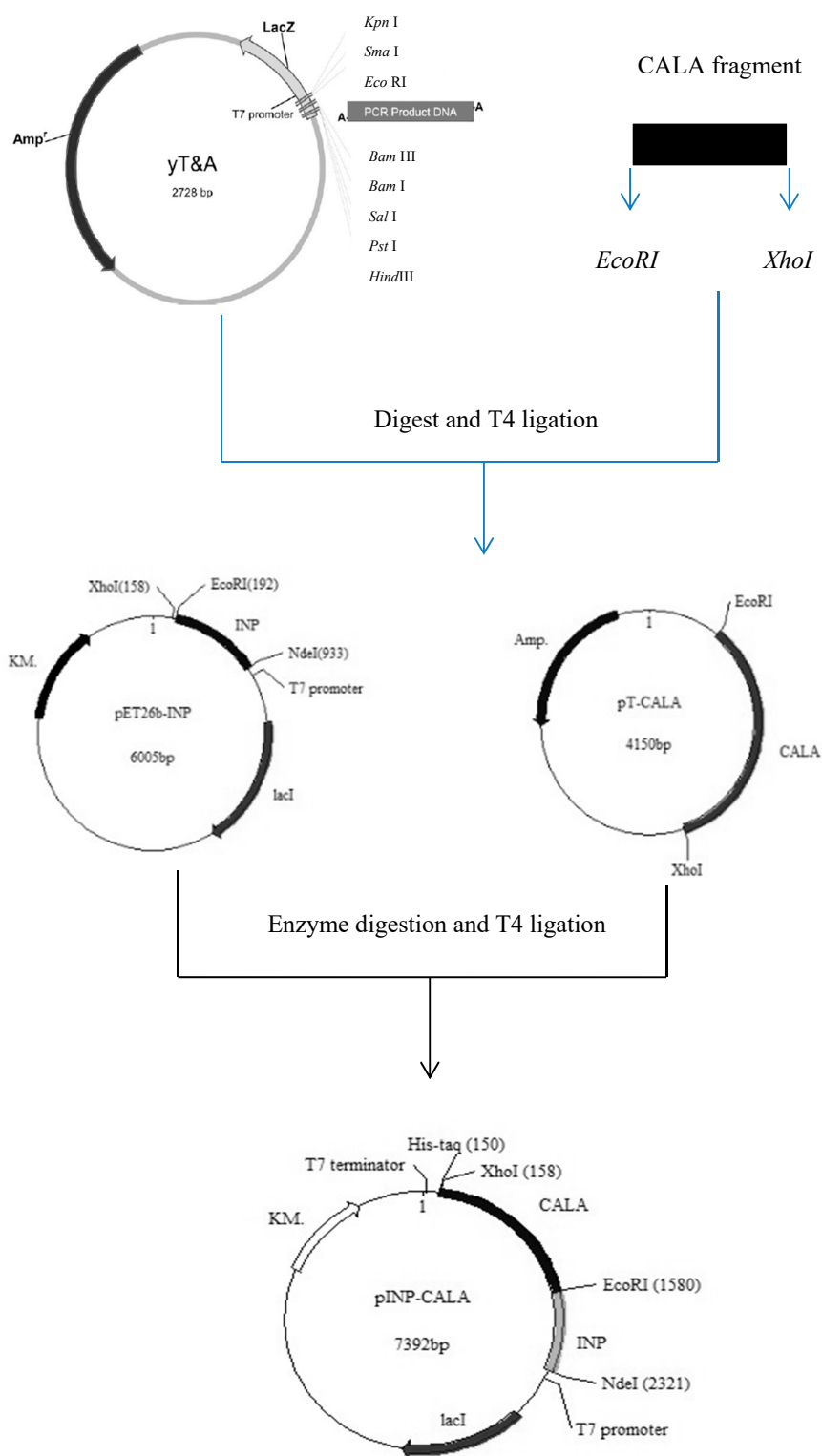


Figure 9. Construction of pINP-CALA.

3.3. Cultivation Conditions

E. coli JM109 strains carrying *cala* and *inaX-cala* genes were activated from the preservation freezer to a Petri dish with Luria-Bertani (LB) agar plus 10 μ L (50 mg/mL) ampicillin and cultured at 37 °C for 12 h. A single colony was picked to inoculate 10 mL LB medium plus 10 μ L (50 mg/mL) ampicillin; the culture was operated at 37 °C and a shaking rate of 200 rpm for 12 h. A volume of 1% seed culture was used to inoculate 100 mL of LB medium plus 100 μ L (50 mg/mL) ampicillin. Cultivation was conducted at 37 °C and 200 rpm until the cell optical density (OD₆₀₀) reached 0.8, followed by the addition of isopropyl β -D-1-thiogalactopyranoside (IPTG) to a final concentration of 0.1 mM. The cultivation temperature and time were set at 15 °C and 24 h, respectively, while the shaking rate was varied from 50 to 200 rpm. To prepare CALA, the broth was centrifuged at 3000 g for 10 min to collect the cells. The cells were subjected to sonication disruption (ultrasonic processing at 20 W for 10 cycles: 30 s working, 30 s free) and centrifugation (10,000 g, 10 min) to separate the supernatant from the cell debris pellet. Both samples were subjected to a dyeing process prior to performing the SDS-PAGE assay. The dyeing solution comprised 10% SDS, 50% glycerol, 1.5 M Tris-Cl (pH 6.8), 2% β -mercaptoethanol, and 0.5% bromophenol blue. The samples were mixed with the dyeing solution at a ratio of 5:1, followed by heating at 100 °C for 10 min, to give the loading samples for SDS-PAGE. To prepare the whole-cell sdCALA, centrifugation (3000 g, 10 min) was applied to separate the cells from the broth; the cells were resuspended in phosphate buffer (pH 6.0) for use in all of the enzyme tests.

3.4. Estimation of Shear Stress and Mass Transfer Coefficient

The oxygen mass transfer coefficient (K_{La}) for an Erlenmeyer flask can be estimated according to the following equation described by Sanchez et al. [41]:

$$K_{La} = 0.024n^{1.16}V_L^{-0.83}d_0^{0.38}d^{1.92} \quad (1)$$

where n is the rate (rpm); V_L is the liquid volume in the shake flask (ml); d_0 is the incubator shaking diameter (cm); and d is the maximal diameter of the shake flask (cm). The units of K_{La} are (h^{-1}).

The average shear rate (γ) and shear stress (τ_t) of a liquid in a shake flask can be estimated using the following formulas [42].

$$\gamma = 3600 \frac{\tau_t}{\mu_L} \quad (2)$$

$$\tau_t = 0.0676 \left(\frac{d_p}{\lambda} \right)^2 (\rho_L \mu_L \varepsilon)^{0.5} \quad (3)$$

where ρ_L is the density of the liquid (kg/m^3), μ_L is the viscosity of the liquid (Pas), d_p is the average cell diameter (m), λ is the Kolmogorov length scale (m), and ε is the energy dissipation rate (m^2/s^3), which are calculated from the following equation:

$$\lambda = \left(\frac{\mu_L}{\rho_L} \right)^{3/4} \varepsilon^{-1/4} \quad (4)$$

$$\varepsilon = \frac{1.94n^{2.8}d_s^{3.6}\mu_L^{0.2}}{V_L^{2/3}\rho_L^{0.2}} \quad (5)$$

where n is the rate (1/s), d_s is the flask diameter (m), and V_L is the working volume of the medium (m^3). The units of γ are (h^{-1}); the units of τ_t are (N/m^2).

3.5. Kinetics Models

The kinetics were derived from the Michaelis–Menten equation as follows:

$$v = \frac{v_m S}{K_m + S} \quad (6)$$

Rearranging Equation (6) by inversion and multiplication by S yields the Hanes–Wolf equation

$$\frac{S}{v} = \frac{1}{v_m} S + \frac{K_m}{v_m} \quad (7)$$

where S is the initial substrate concentration, v is the reaction rate, K_m is the Michaelis–Menten constant, and v_m is the maximum reaction rate. The Hanes–Wolf equation was applied by plotting S/v with respect to S , to yield a straight line of slope $1/v_m$ and an intercept of K_m/v_m .

Lipase hydrolysis reactions were performed to estimate the reaction rate constants. In the tests, the initial activities of CALA and sdCALA were set at 0.35 U/mL, while the concentration of p-NPP was varied from 0.1 to 10 mg/mL (equivalent to 0.265–26.5 $\mu\text{mol/mL}$). The activity measured at 60 °C and pH 6 was used to represent the sample reaction rate [43].

3.6. Assays

Protein analysis was performed using 15% SDS-PAGE and Coomassie Blue staining [44]. The lipase activity was assayed using the modified method described by Chiou et al. [43]. A 50% ethanol solution of the reaction mixture was prepared as follows: 0.1 mL of free lipase was added to a mixture of 1 mL of p-NPP (5 mg/mL in 99% ethanol) and 1 mL of 50 mM phosphate buffer (pH 6.0), followed by incubating at 60 °C and 100 rpm for 5 min. The reaction was terminated by adding 0.9 mL of 0.5 N Na_2CO_3 to a 0.1 mL sample; all of the samples were centrifuged at 10,000 g for 15 min. The absorbance of the supernatant at 410 nm was measured using a UV–Vis spectrophotometer (Beckman DU-530, Fullerton, CA, USA). A molar extinction coefficient for *p*-nitrophenol of 15,000 $\text{M}^{-1} \text{cm}^{-1}$ was used. Unless stated otherwise, one unit (1U) of enzyme activity was defined as the amount of enzyme required to produce 1 μmol of *p*-nitrophenol per min at 60 °C and pH 6.0.

For the thermal stability tests, 1 mL of sdCALA (0.35 U/mL) was heated on an incubator set at 37–90 °C for 30 min, followed by cooling in an ice bath to remove the residual heat. The sdCALA activity was measured at 60 °C and pH 6 for 5 min. For the organic solvent tests, the reaction substrate (p-NPP) was dissolved in various concentrations of ethanol, isopropanol, acetone, and acetonitrile, and then the activity was measured at 60 °C and pH 6 for 5 min. Tributyrin agar plate tests were based on the method described by Jung et al. [45]. A drop (10 μL) of the harvested broth was placed on a prepared tributyrin agar plate and left at room temperature for 3 days; then, the clear zone around the tested sample was scrutinized.

3.7. Statistical Analysis

To obtain statistical results, all data were analyzed using Origin software (v. 9.0). Experiments were performed in triplicate and data are expressed as means \pm SD; significant differences between means were identified through analysis of variance (Origin software, v.9.0).

4. Conclusions

We have observed that the shaking rate has an effect on the production of surface-displayed lipase A. Since sdCALA was exposed outside the cell membrane, an increase in the shaking rate during cultivation had a negative effect on this surface-displayed enzyme. Indeed, the increased shaking rate lowered the specific activity of sdCALA as a result of shear stress. In contrast, the cultivation conditions did not affect the temperature and pH dependency of CALA and sdCALA. A kinetic study revealed that the cultivation of sdCALA at a moderate shaking rate optimized the hydrolysis performance.

Furthermore, the observed decrease in the specific activity of sdCALA in the presence of various organic solvents was presumably due to the effect of decomposition of the host cells.

Author Contributions: Data curation and methodology, C.-F.C. and S.-C.L., conceptualization, writing—original draft preparation; writing—review and editing, project administration, T.-Y.J. and Y.-C.L. All authors have read and agreed to the published version of the manuscript.

Funding: This study was supported by research grants from the National Science Council of Taiwan (grant nos. MOST 103-2221-E-005-071-MY3 and MOST 106-2313-B-005-029) and China Medical University (grant nos. CMU108-AWARD-01 and CMU-108-MF-122).

Conflicts of Interest: The authors declare no conflicts of interest.

References

1. Kirk, O.; Christensen, M.W. Lipases from *Candida antarctica*: Unique biocatalysts from a unique origin. *Org. Process Res. Dev.* **2002**, *6*, 446–451. [[CrossRef](#)]
2. Uppenberg, J.; Parkar, S.; Bergfors, T.; Jones, T.A. Crystallization and preliminary X-ray studies of lipase B from *Candida antarctica*. *J. Mol. Biol.* **1994**, *235*, 790–792. [[CrossRef](#)] [[PubMed](#)]
3. Blank, K.; Morfill, J.; Gump, H.; Gaub, H.E. Functional expression of *Candida antarctica* lipase B in *Escherichia coli*. *J. Biotechnol.* **2006**, *125*, 474–483. [[CrossRef](#)] [[PubMed](#)]
4. Widmann, M.; Juhl, P.B.; Pleiss, J. Structural classification by the lipase engineering database: A case study of *Candida antarctica* lipase A. *BMC Genom.* **2010**, *11*, 123–131. [[CrossRef](#)]
5. de María, P.D.; Carboni-Oerlemans, C.; Tuin, B.; Bargeman, G.; van der Meer, A.; van Gemert, R. Biotechnological applications of *Candida antarctica* lipase A: State-of-the-art. *J. Mol. Catal. B-Enzym.* **2005**, *37*, 36–46. [[CrossRef](#)]
6. Hoegh, I.; Patkar, S.; Halkier, T.; Hansen, M.T. Two lipases from *Candida antarctica*: Cloning and expression in *Aspergillus oryzae*. *Can. J. Bot.* **1995**, *73*, 869–875. [[CrossRef](#)]
7. Pfeffer, J.; Richter, S.; Nieveler, J.; Hansen, C.E.; Rhlid, R.B.; Schmid, R.D.; Rusnak, M. High yield expression of lipase A from *Candida antarctica* in the methylotrophic yeast *Pichia pastoris* and its purification and characterisation. *Appl. Microbiol. Biotechnol.* **2006**, *72*, 931–938. [[CrossRef](#)]
8. Pfeffer, J.; Rusnak, M.; Hansen, C.-E.; Rhlid, R.B.; Schmid, R.D.; Maurer, S.C. Functional expression of lipase A from *Candida antarctica* in *Escherichia coli*—A prerequisite for high-throughput screening and directed evolution. *J. Mol. Catal. B-Enzym.* **2007**, *45*, 62–67. [[CrossRef](#)]
9. Larsen, M.W.; Bornscheuer, U.T.; Hult, K. Expression of *Candida antarctica* lipase B in *Pichia pastoris* and various *Escherichia coli* systems. *Protein Expr. Purif.* **2008**, *62*, 90–97. [[CrossRef](#)]
10. Larios, A.; Garcia, H.S.; Oliart, R.M.; Valerio-Alfaro, G. Synthesis of flavor and fragrance esters using *Candida antarctica* lipase. *Appl. Microbiol. Biotechnol.* **2004**, *65*, 373–376. [[CrossRef](#)]
11. Ognjanovic, N.; Bezbradica, D.; Knezevic-Jugovic, Z. Enzymatic conversion of sunflower oil to biodiesel in a solvent-free system: Process optimization and the immobilized system stability. *Bioresour. Technol.* **2009**, *100*, 5146–5154. [[CrossRef](#)]
12. Smith, G.P. Filamentous phage—novel expression vectors that display cloned antigens on the virion surface. *Science* **1985**, *228*, 1315–1317. [[CrossRef](#)] [[PubMed](#)]
13. Lee, S.Y.; Choi, J.H.; Xu, Z. Microbial cell-surface display. *Trends Biotechnol.* **2003**, *21*, 45–52. [[CrossRef](#)]
14. Wernerus, H.; Stahl, S. Biotechnological applications for surface engineered bacteria. *Biotechnol. Appl. Biochem.* **2004**, *40*, 209–228. [[PubMed](#)]
15. Margaritis, A.; Bassi, A.S. Principles and biotechnological applications of bacterial ice nucleation. *Crit. Rev. Biotechnol.* **1991**, *11*, 277–295. [[CrossRef](#)] [[PubMed](#)]
16. Edwards, A.R.; Van Den Bussche, R.A.; Wichman, H.A.; Orser, C.S. Unusual pattern of bacterial ice nucleation gene evolution. *Mol. Biol. Evol.* **1994**, *11*, 911–920.
17. van Bloois, E.; Winter, R.T.; Kolmar, H.; Fraaije, M.W. Decorating microbes: Surface display of proteins on *Escherichia coli*. *Trends Biotechnol.* **2011**, *29*, 79–86. [[CrossRef](#)]
18. Samuelson, P.; Gunneriusson, E.; Nygren, P.A.; Stahl, S. Display of proteins on bacteria. *J. Biotechnol.* **2002**, *96*, 129–154. [[CrossRef](#)]
19. Li, Q.; Yu, Z.; Shao, X.; He, J.; Li, L. Improved phosphate biosorption by bacterial surface display of phosphate binding protein utilizing ice nucleation protein. *FEMS Microbiol. Lett.* **2009**, *299*, 44–52. [[CrossRef](#)]

20. Shimazu, M.; Mulchandani, A.; Chen, W. Cell surface display of organophosphorus hydrolase using ice nucleation protein. *Biotechnol. Prog.* **2001**, *17*, 76–80. [[CrossRef](#)]
21. Wu, P.H.; Giridhar, R.; Wu, W.T. Surface display of transglucosidase on *Escherichia coli* by using the ice nucleation protein of *Xanthomonas campestris* and its application in glucosylation of hydroquinone. *Biotechnol. Bioeng.* **2006**, *95*, 1138–1147. [[CrossRef](#)] [[PubMed](#)]
22. Matsumoto, T.; Fukuda, H.; Ueda, M.; Tanaka, A.; Kondo, A. Construction of yeast strains with high cell surface lipase activity by using novel display systems based on the Flo1p flocculation functional domain. *Appl. Environ. Microbiol.* **2002**, *68*, 4517–4522. [[CrossRef](#)] [[PubMed](#)]
23. Moura, M.V.H.; Silva, G.P.D.; Machado, A.C.D.O.; Torres, F.A.G.; Freire, D.M.G.; Almeida, R.V. Displaying lipase B from *Candida antarctica* in *Pichia pastoris* using the yeast surface display approach: Prospection of a new anchor and characterization of the whole cell biocatalyst. *PLoS ONE* **2015**, *12*, e0141454. [[CrossRef](#)] [[PubMed](#)]
24. Liu, W.; Zhao, H.; Jia, B.; Xu, L.; Yan, Y. Surface display of active lipase in *Saccharomyces cerevisiae* using Cwp2 as an anchor protein. *Biotechnol. Lett.* **2010**, *32*, 255–260. [[CrossRef](#)]
25. Wilhelm, S.; Rosenau, F.; Becker, S.; Buest, S.; Hausmann, S.; Kolmar, H.; Jaeger, K.-E. Functional cell-surface display of a lipase-specific chaperone. *Chembiochem* **2007**, *8*, 55–60. [[CrossRef](#)]
26. Jo, J.-H.; Han, C.-W.; Kim, S.-H.; Kwon, H.-J.; Lee, H.-H. Surface display expression of *Bacillus licheniformis* lipase in *Escherichia coli* using Lpp'OmpA Chimera. *J. Microbiol.* **2014**, *52*, 856–862. [[CrossRef](#)]
27. Kan, S.-C.; Chen, C.-M.; Lin, C.-C.; Wu, J.-Y.; Shieh, C.-J.; Liu, Y.-C. Deciphering EGFP production via surface display and self-cleavage intein system in different hosts. *J. Taiwan Inst. Chem. Eng.* **2015**, *55*, 1–6. [[CrossRef](#)]
28. Lin, C.-C.; Liu, T.-T.; Kan, S.-C.; Zang, C.-Z.; Yeh, C.-W.; Wu, J.-Y.; Chen, J.-H.; Shieh, C.-J.; Liu, Y.-C. Production of D-Hydantoinase via surface display and self-cleavage system. *J. Biosci. Bioeng.* **2013**, *116*, 562–566. [[CrossRef](#)]
29. Wu, J.-Y.; Chen, C.-I.; Chen, C.-M.; Lin, C.-C.; Kan, S.-C.; Shieh, C.-J.; Liu, Y.-C. Cell disruption enhanced the pure EGFP recovery from an EGFP-intein- surface protein production system in recombinant *E. coli*. *Biochem. Eng. J.* **2012**, *68*, 12–18. [[CrossRef](#)]
30. Wu, J.-Y.; Tsai, T.-Y.; Liu, T.-T.; Lin, C.-C.; Chen, J.-H.; Yang, S.-C.; Shieh, C.-J.; Liu, Y.-C. Production of recombinant EGFP via surface display of ice nucleation protein and self-cleavage intein. *Biochem. Eng. J.* **2011**, *54*, 158–163. [[CrossRef](#)]
31. Shamel, M.M.; Ramachandran, K.B.; Hasan, M. Operational stability of lipase enzyme: Effect of temperature and shear. *Dev. Chem. Eng. Min. Process.* **2005**, *13*, 599–604. [[CrossRef](#)]
32. Dimitrijevic, A.; Velickovic, D.; Bihelovic, F.; Bezbradica, D.; Jankov, R.; Milosavic, N. One-step, inexpensive high yield strategy for *Candida antarctica* lipase A isolation using hydroxyapatite. *Bioresour. Technol.* **2012**, *107*, 358–362. [[CrossRef](#)] [[PubMed](#)]
33. Zamost, B.L.; Nielsen, H.K.; Starnes, R.L. Thermostable enzymes for industrial applications. *J. Ind. Microbiol.* **1991**, *8*, 71–81. [[CrossRef](#)]
34. Panpipat, W.; Xu, X.; Guo, Z. Improved acylation of phytosterols catalyzed by *Candida antarctica* lipase A with superior catalytic activity. *Biochem. Eng. J.* **2013**, *70*, 55–62. [[CrossRef](#)]
35. Boran, R.; Ugur, A. Partial purification and characterization of the organic solvent-tolerant lipase produced by *Pseudomonas fluorescens* RB02-3 isolated from milk. *Prep. Biochem. Biotechnol.* **2010**, *40*, 229–241. [[CrossRef](#)] [[PubMed](#)]
36. El-Batal, A.I.; Farrag, A.A.; Elsayed, M.A.; El-Khawaga, A.M. Effect of environmental and nutritional parameters on the extracellular lipase production by *Aspergillus niger*. *Int. Lett. Nat. Sci.* **2016**, *60*, 18–29. [[CrossRef](#)]
37. Yang, C.; Wang, F.; Lan, D.; Whiteley, C.; Yang, B.; Wang, Y. Effects of organic solvents on activity and conformation of recombinant *Candida antarctica* lipase A produced by *Pichia pastoris*. *Process Biochem.* **2012**, *47*, 533–537. [[CrossRef](#)]
38. Ramos, J.L.; Duque, E.; Rodríguez-Herva, J.J.; Godoy, P.; Haïdour, A.; Reyes, F.; Fernández-Barrero, A. Mechanisms for solvent tolerance in bacteria. *J. Biol. Chem.* **1997**, *272*, 3887–3890. [[CrossRef](#)]
39. Segura, A.; Duque, E.; Mosqueda, G.; Ramos, J.L.; Junker, F. Multiple responses of Gram-negative bacteria to organic solvents. *Environ. Microbiol.* **1999**, *1*, 191–198. [[CrossRef](#)]
40. Sambrook, J.; Russel, D.W. *Molecular Cloning: A Laboratory Manual*, 3rd ed.; Cold Spring Harbor Laboratory Press: New York, NY, USA, 2001.

41. Sanchez, C.E.G.; Martinez-Trujillo, A.; Osorio, G.A. Oxygen transfer coefficient and the kinetic parameters of exo-polygalacturonase production by *Aspergillus flavipes* FP-500 in shake flasks and bioreactor. *Lett. Appl. Microbiol.* **2012**, *55*, 444–452. [[CrossRef](#)]
42. Camacho, F.G.; Rodriguez, J.J.G.; Miron, A.S.; Garcia, M.C.C.; Belarbi, E.H.; Grima, E.M. Determination of shear stress thresholds in toxic dinoflagellates cultured in shaken flasks Implications in bioprocess engineering. *Process Biochem.* **2007**, *42*, 1506–1515. [[CrossRef](#)]
43. Chiou, S.H.; Wu, W.T. Immobilization of *Candida rugosa* lipase on chitosan with activation of the hydroxyl groups. *Biomaterials* **2004**, *25*, 197–204. [[CrossRef](#)]
44. Laemmli, U.K. Cleavage of structural proteins during the assembly of the head of bacteriophage T4. *Nature* **1970**, *227*, 680–685. [[CrossRef](#)] [[PubMed](#)]
45. Jung, H.C.; Ko, S.; Ju, S.J.; Kim, E.J.; Kim, M.K.; Pan, J.G. Bacterial cell surface display of lipase and its randomly mutated library facilitates high-throughput screening of mutants showing higher specific activities. *J. Mol. Catal. B-Enzym.* **2003**, *26*, 177–184. [[CrossRef](#)]



© 2020 by the authors. Licensee MDPI, Basel, Switzerland. This article is an open access article distributed under the terms and conditions of the Creative Commons Attribution (CC BY) license (<http://creativecommons.org/licenses/by/4.0/>).